Sustainable Energy & Fuels

ROYAL SOCIETY OF CHEMISTRY

PAPER

View Article Online
View Journal | View Issue

Cite this: *Sustainable Energy Fuels*, 2021, **5**, 2504

Economic and life-cycle assessment of OME_{3-5} as transport fuel: a comparison of production pathways†

Daniel F. Rodríguez-Vallejo, [a] Antonio Valente, ‡[b] Gonzalo Guillén-Gosálbez *[b] and Benoît Chachuat [a]

Reducing the contribution of the transport sector to climate change calls for a transition towards renewable fuels. Polyoxymethylene dimethyl ethers (OME_n) constitute a promising alternative to fossil-based diesel. This article presents a comparative analysis of 17 OME_{3-5} production pathways, benchmarked against fossil-based diesel under environmental and economic criteria following a life-cycle approach. OME_{3-5} fuels that are reliant on biomass as feedstock, or use H_2 produced from wind- or nuclear-powered electrolysis and CO_2 from direct air capture, have the potential to reduce global warming impacts by up to 20%. Nevertheless, such fuels are also found to shift environmental burdens to other impact categories under human health and ecosystems quality due to procurement of raw materials (H_2, CO_2 and biomass), and their predicted total monetized cost is 1.5–3.6 times that of fossil-based diesel. These results highlight the need for embracing impacts beyond climate change in the environmental assessment of alternative fuels and including negative externalities in their economic assessment.

Received 6th March 2021
Accepted 24th March 2021

DOI: 10.1039/d1se00335f

rsc.li/sustainable-energy

1 Introduction

The past few decades have witnessed considerable debate around anthropogenic climate change. The current levels of carbon dioxide (CO_2) and other greenhouse gas (GHG) emissions raise major concerns on global warming and climate change, in response to which a growing number of programs and initiatives are being pursued.[1]

The transport sector—which primarily involves road, rail, air and marine transportation—is among the major contributors to climate change, representing around 14% of global GHG emissions and around 25% of global CO_2 emissions from fossil fuels.[2–4] In 2017 it was estimated that oil consumption for the transport sector alone amounted to 188.7 quad Btu (quadrillion of British thermal units), making up 60% of the global oil demand. This scenario is expected to continue for the next 30 years with gasoline and diesel remaining the prominent fuels.[5] By contrast, the energy consumption of the transport sector per unit of GDP has decreased by 1.4% per year between 2000 and 2018 on average. But this value remains well below the average reduction of 3.2% per year targeted by the International Energy Agency (IEA) over the period 2020–2030 to limit the global temperature increase to below 2 °C.[4] Reducing the negative effects of the transport sector emissions further in order to meet these sustainability targets, therefore, calls for a transition toward renewable fuels.[6]

The production of alternative fuels *via* the catalytic conversion of renewable-based hydrogen (H_2) and CO_2 represents a promising path towards defossilization of the transport sector.[6] Examples of fuels derived from the catalytic conversion of CO_2 include methane, methanol and its conversion to gasoline, dimethyl ether (DME) and, more recently, polyoxymethylene dimethyl ethers (OME), which are the focus of this study.

OMEs are oligomers with the general chemical structure CH_3–O–$(CH_2O)_n$–CH_3. Apart from their utilization as a transport fuel, OMEs are also employed as physical solvent for the absorption of CO_2 in natural gas processing, green solvent in the chemical industry, and fuel for direct oxidation in fuel cells.[7] It has been reported that OME can be used directly in conventional compression ignition engines with minor or even no modifications.[8–11] The need for blending OMEs with fossil-based diesel depends on the oligomerization chain length n. OME_1 ($n = 1$) – also known as methylal – requires blending with fossil-based diesel since its vapour pressure and boiling point (42 °C) are comparable to those of other gaseous fuels.[6] By contrast, OME_{3-5} ($3 \leq n \leq 5$) has a lower vapour pressure and higher boiling point (*cf.* 200 °C).[10] It can be transported and distributed through the conventional diesel infrastructure and

[a]*The Sargent Centre for Process Systems Engineering, Imperial College London, South Kensington Campus, SW7 2AZ London, UK*

[b]*Institute for Chemical and Bioengineering, Swiss Federal Institute of Technology, Vladimir-Prelog-Weg 1, 8093 Zurich, Switzerland. E-mail: gonzalo.guillen.gosalbez@chem.ethz.ch*

† Electronic supplementary information (ESI) available. See DOI: 10.1039/d1se00335f

‡ Current address: European Commission, Joint Research Centre, Directorate D, Via Enrico Fermi 2749, 21027 Ispra, Italy.

be directly used in diesel engines without blending. Other benefits of OME fuels include reduced soot and indirect NO_x formation during their combustion in diesel engines,[6,7] better auto-ignition capabilities than alcohols, better stability than fatty acid methyl esters (biodiesel), and superior volatility affinity to diesel than DME and dymethoxymethane.[8]

The synthesis of OME_{3-5} requires a source of methyl groups and a source of formaldehyde (FA). The former is usually obtained from methanol, DME or methylal; the latter can be obtained from methanol–FA–water solutions, paraformaldehyde or trioxane. The two main catalytic routes for the synthesis of OME are: (1) the reaction between trioxane and methylal,[12] which are produced from FA and methanol, respectively; and (2) the direct reaction between FA and methanol.[6,13] The first route does not generate water, while the direct route co-produces water with OME_{3-5} to avoid the trioxane and methylal intermediates.[7]

Given the relevance of OME_{3-5} as a transportation fuel substitute, it is important to accurately quantify its environmental performance. The standardised methodology of life-cycle assessment (LCA)[14,15] can be used to conduct this analysis by following a holistic approach. LCA quantifies the potential environmental impacts across different life-cycle stages (cradle-to-grave approach) by taking into account both upstream and downstream processes.[16–20]

Deutz *et al.*[6] conducted a well-to-wheel assessment of a diesel blend comprising 24% (mass) of OME_1. They considered OME_1 produced from the catalytic reaction between renewable H_2 from electrolysis and CO_2 captured from biogas or direct air capture (DAC). They quantified the global warming (GW), NO_x and soot emissions as well as the cumulative energy demand (CED). Their results showed that, compared to fossil-based diesel, the OME_1-diesel blend could reduce the GW, NO_x and soot by 22%, 43% and 75%, respectively, while the CED was double that of diesel. Hank *et al.*[13] compared the environmental performance of OME_{3-5} produced from renewable H_2 and CO_2 captured from biogas, ammonia plants or DAC to fossil-based diesel. Their assessment included the impact categories of GW, acidification, eutrophication, respiratory effects, photochemical ozone creation, and resource depletion. They found that OME_{3-5} could reduce the GW by 89%, yet impacts in other categories were predicted to significantly exceed those of fossil-based diesel. Other studies have considered the techno-economics of OME_1 production,[21] the conceptual process design and analysis of OME plants,[7,12,22–27] the physicochemical characterization and kinetic modelling of OME,[28–33] and the combustion emissions associated to the use of OME fuels in compression ignition engines.[8,34]

By and large, studies assessing the environmental performance of OME_{3-5} are indeed scarce. The focus so far has been on specific impact categories, mainly GW and NO_x formation, while other relevant impact categories related to human health, ecosystem quality, and resource availability have not been quantified. Omitting impacts beyond climate change may only provide an incomplete picture and, ultimately, could even be misleading regarding the real potential of OME_{3-5} as a sustainable substitute to fossil-based diesel.

Bearing the above in mind, this article presents a comprehensive environmental assessment of multiple OME_{3-5} production pathways, complemented by a full cost analysis accounting for their monetized environmental impacts (externalities). To our knowledge, this is the first OME assessment with such breadth (17 production pathways) and depth (3 endpoint LCA indicators, including externalities). The environmental performance is quantified through the LCA methodology, and the economic performance is expressed in terms of the driving cost (DC). Monetization factors are applied to the environmental impacts to explore their potential economic implications. These 17 pathways are furthermore benchmarked against fossil-based diesel.

The remainder of this paper is structured as follows: Section 2 presents the methodology employed in the environmental assessment of the OME_{3-5} fuels, including a description of the LCA methodology, the definition of the case study and computation of the impact indicators employed. The results of the assessment are presented and discussed in Section 3, before drawing conclusions in Section 4.

2 Materials and methods

This study quantifies the environmental and economic life-cycle performance of 17 OME_{3-5} production routes as potential alternatives to conventional diesel. Methanol, a common intermediate to all 17 routes, is either derived from steam methane reforming (SMR), from synthesis gas (syngas) produced by biomass gasification (BTM), or from CO_2 hydrogenation (catalytic reaction of renewable-based H_2 with CO_2 captured from industrial flue gas or directly from air).

2.1 Life-cycle assessment

LCA is a well-established methodology for quantifying the environmental burdens associated with products, processes or activities across their life-cycle.[17,35] It is also a prominent tool for guiding sustainable product and process design. LCA can be used to evaluate the environmental performance of any product, process or activity, following a cradle-to-grave approach—from extraction and processing of raw materials to recycling and final disposal. LCA furthermore aggregates the environmental burdens under a set of impact categories and indicators that can be easily understood and communicated to inform decision- and policy-making.[17,18] The methodological framework of LCA (Fig. 1) comprises four interconnected phases with information exchange between them:[14,15]

2.1.1 Goal and scope definition. This phase defines the main intent of the study, the target audience, the time and geographical coverage, the boundaries of the system (*e.g.*, cradle-to-gate, well-to-wheel), the functional unit (*i.e.*, the reference unit associated with the main function of the system under analysis), and the impact categories.

2.1.2 Life-cycle inventory analysis (LCI). This phase quantifies the main input and output flows (*i.e.*, emissions, wastes, energy, and raw materials) crossing the system's boundaries relative to the functional unit.

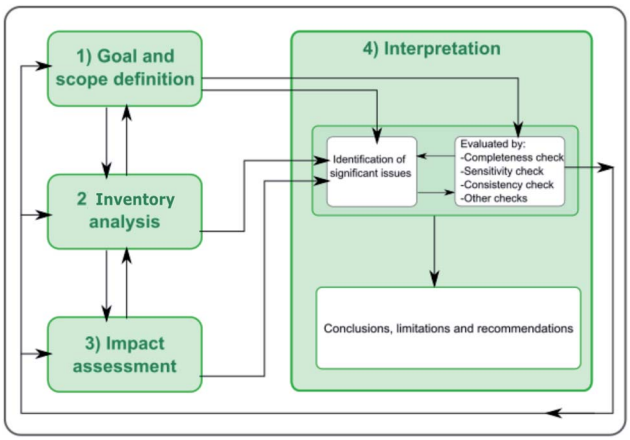

Fig. 1 Life cycle assessment phases.

2.1.3 Life-cycle impact assessment (LCIA). This phase comprises a classification stage where the elementary flows are assigned to the selected impact categories; followed by a characterization stage for converting elementary emissions into impacts. This entails the application of a set of characterization factors that are specific to the assessment method (*e.g.*, ReCiPe, EF, CML, IPCC) and to the impact category (*e.g.*, GW, acidification, eutrophication). Normalization and weighting are optional stages, which enable the aggregation of different impact categories under a single environmental performance score.

2.1.4 Interpretation. This final phase summarizes the findings from both LCI and LCIA phases, seeks to identify the critical life-cycle stages, and analyzes the sensitivity of key parameters. This leads to recommendations for improving the environmental performance of the system of interest.

2.2 LCA model definition

2.2.1 Goal and scope definition. In order to compare the environmental performance of the OME_{3-5} fuels with fossil-based diesel, the functional unit of the LCA is chosen as "*1 kilometer travelled*". The assessment of OME_{3-5} entails the analysis of four interconnected subsystems with exogenous energy and material flows (Fig. 2). Further details on the

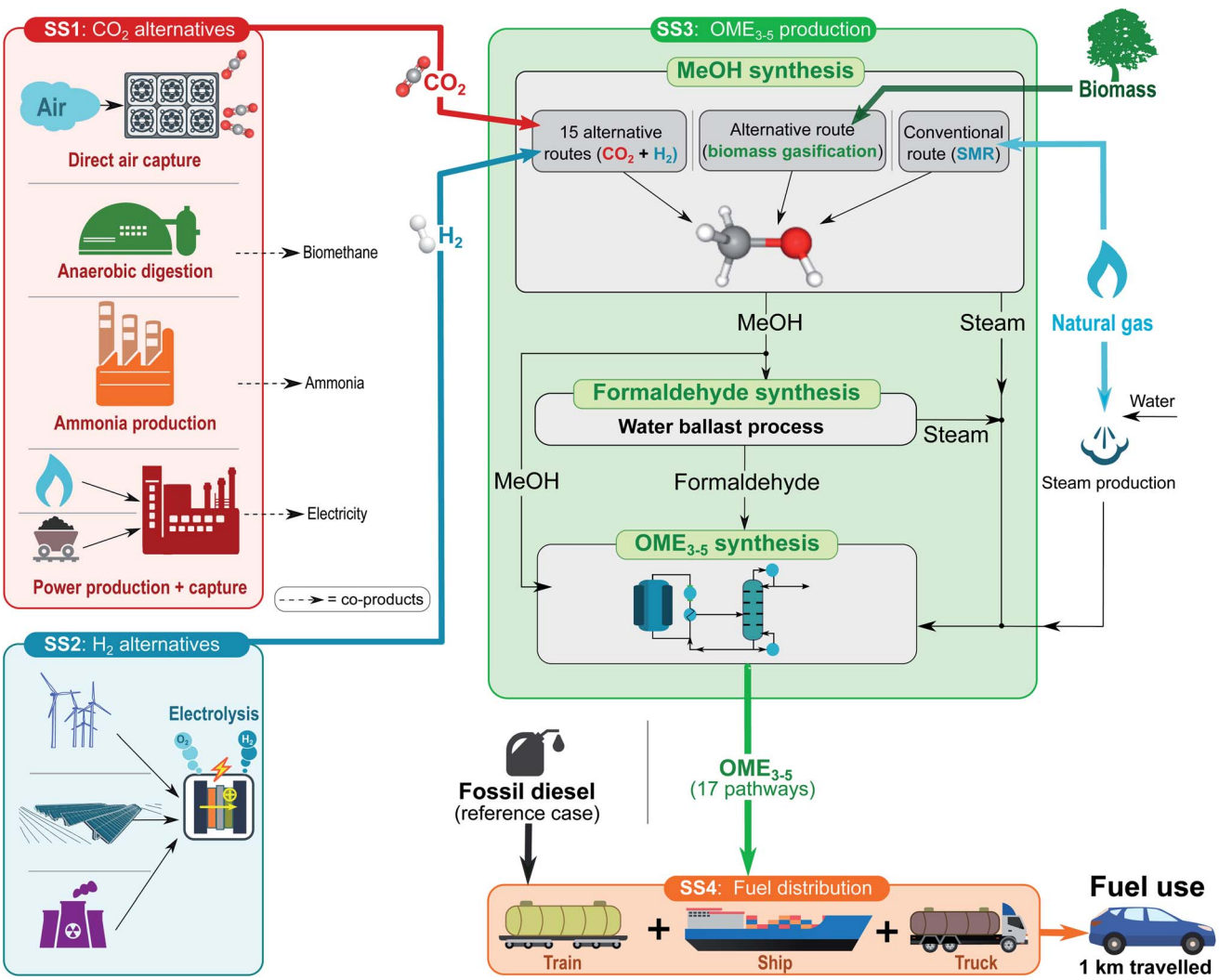

Fig. 2 Scope of the OME_{3-5} infrastructure divided in CO_2 (SS1), H_2 (SS2), OME_{3-5} (SS3), and utilization (SS4) subsystems.

modeling assumptions for each subsystem are given in Section 2.2.2.

2.2.1.1 CO_2 alternatives. Subsystem SS1 is concerned with the procurement of CO_2 (red box). Five alternatives are considered as possible sources of CO_2: (i) direct air capture (DAC), (ii) anaerobic digestion of sewage sludge, (iii) ammonia production, and (iv) gas- or (v) coal-fired power plants. Apart from DAC, all of these processes are multi-product, which requires dealing with multi-functionality.

The CO_2 used as feedstock may be described in either one of two ways.[36,37] When considered a valuable product stream, the CO_2 capture process becomes multi-functional since it procures CO_2 in addition to the main product—either biomethane, ammonia or electricity depending on the CO_2 capture point-source (see SS1 in Fig. 2). When considered a waste stream, the same CO_2 capture process is mono-functional, but the utilization stage (*cf.* SS3 in Fig. 2) becomes multi-functional since it now recycles a waste stream into a valuable product (OME_{3-5}). We shall adopt the former viewpoint subsequently by treating CO_2 capture as a multi-functional process.

The recommended ISO standard[14,15] for handling multi-functionality is system subdivision, whereby a multi-functional system is split into multiple mono-functional systems that are assessed separately. Where system subdivision is not possible, impact allocation procedures may still be avoided *via* system expansion, whereby co-products displace the burdens associated with the corresponding marketable product generated through the conventional pathway. And where neither system subdivision nor system expansion is possible, allocation may be applied to distribute all the inputs and outputs among the co-products based on physical or economic criteria (*e.g.*, mass, energy, exergy, carbon content, or monetary value).

Because our assessment is product-specific and aims to express the impacts per kilometer travelled, neither system subdivision nor system expansion is readily applicable. The avoided burden approach is also impractical since (i) there is no guarantee that a mono-functional process is always available for environmental credits and (ii) the environmental benefits are not distributed among the functions but solely assigned to one functional unit, which would make the analysis ambiguous. By contrast, allocation can in principle support a fair distribution of the environmental benefits and impacts among various functions in CCU applications.[37,38] For these reasons, an allocation approach based on economic criteria is adopted subsequently.

The economic value of CO_2 varies greatly among authors, with prices reported in the range of €40–650 per ton CO_2,[36,39] and several authors arguing in favor of a zero or even negative price for concentrated CO_2 in the future.[36,39,40] However, there is a lack of clarity as to how the price of concentrated CO_2 might evolve if it were to become widely available. Given this uncertainty, the economic allocation herein is based on the estimated cost of CO_2 capture for each point-source (anaerobic digestion, ammonia production, or power generation). A sensitivity analysis of the environmental impacts with respect to this capture cost is conducted later on in Section 3.

2.2.1.2 H_2 alternatives. Subsystem SS2 involves the production of H_2 (blue box). Three alternative hydrogen production pathways are considered: PEM electrolysis powered by (i) wind-, (ii) solar-, and (iii) nuclear-based electricity. Allocation is not needed since H_2 is the only product of this subsystem.

2.2.1.3 OME_{3-5} production. Subsystem SS3 is concerned with OME_{3-5} production (green box) and comprises three sections for the production of methanol, formaldehyde and OME_{3-5}. Methanol is either produced *via* SMR, syngas from BTM, or catalytic CO_2 hydrogenation – with CO_2 and H_2 from SS1 and SS2, respectively. Part of this methanol is subsequently oxidized to formaldehyde, which then reacts with the remaining methanol to produce OME_{3-5}. Neither of these sections calls for an

Table 1 H_2 and CO_2 sources for each OME_{3-5} fuel scenario. Excepting the fuels produced *via* SMR and BTM, the notation $OME_{i,j}$ refers to the combination between H_2 source *i* and CO_2 source *j*

Scenario code	H_2 source	CO_2 source
$OME_{N,Bg}$	Nuclear-based electrolysis	Biogas
$OME_{N,DAC}$	Nuclear-based electrolysis	Direct air capture
$OME_{N,NH3}$	Nuclear-based electrolysis	Ammonia production
$OME_{N,PwC}$	Nuclear-based electrolysis	Coal-based power plant
$OME_{N,PwNG}$	Nuclear-based electrolysis	Natural gas-based power plant
$OME_{S,Bg}$	Solar-based electrolysis	Biogas
$OME_{S,DAC}$	Solar-based electrolysis	Direct air capture
$OME_{S,NH3}$	Solar-based electrolysis	Ammonia production
$OME_{S,PwC}$	Solar-based electrolysis	Coal-based power plant
$OME_{S,PwNG}$	Solar-based electrolysis	Natural gas-based power plant
$OME_{W,Bg}$	Wind-based electrolysis	Biogas
$OME_{W,DAC}$	Wind-based electrolysis	Direct air capture
$OME_{W,NH3}$	Wind-based electrolysis	Ammonia production
$OME_{W,PwC}$	Wind-based electrolysis	Coal-based power plant
$OME_{W,PwNG}$	Wind-based electrolysis	Natural gas-based power plant
OME_{BTM}[a]		
OME_{SMR}[b]		

[a] OME produced from methanol *via* BTM syngas. [b] OME produced from methanol *via* SMR.

allocation since methanol, formaldehyde and OME_{3-5} are the unique products. A summary of the 17 OME_{3-5} production pathways and their corresponding notation is presented in Table 1.

2.2.1.4 Fuel distribution and use. Subsystem SS4 involves the distribution of OME_{3-5} (orange box) and its combustion in a diesel engine.

2.2.2 Data collection and life-cycle inventory. Table 2 presents the input and output flows considered in the LCI of the OME_{3-5} production (Fig. 2). Any electricity inputs, apart from the electrolytic H_2 production, are based on the UK electricity mix, while steam inputs are specified as heat from steam in the chemical industry. Any CO_2 emissions associated with fossil raw materials are accounted for with positive fossil characterization factors in the LCIA phase, whereas CO_2 emissions from the BTM process are modelled as a biogenic emission source. The process employed to benchmark the various OME_{3-5} fuels is diesel from an average oil refinery in Europe.

Table 2 LCI of the OME_{3-5} system following the methanol production pathway: CO_2 + H_2, SMR and BTM. Inventories expressed per kg OME_{3-5}[a]

Flow	H_2 + CO_2	SMR	BTM
Input			
H_2 (kg)	0.22	—	—
CO_2 (kg)	1.65	—	—
Natural gas (m^3)	—	0.73	—
Wood chips (kg)	—	—	3.74
Cooling water (m^3)	0.20	0.18	0.18
Steam (MJ)	4.55	7.18	7.18
Electricity (kWh)	0.17	0.12	0.20
Water, deionised (kg)	—	0.32	1.25×10^{-3}
Methanol catalyst (kg)	1.25×10^{-5}	1.14×10^{-4}	1.48×10^{-4}
OME catalyst (kg)	4.37×10^{-5}	4.37×10^{-5}	4.37×10^{-5}
Infrastructure (unit)	2.40×10^{-10}	2.40×10^{-10}	2.40×10^{-10}
Output[b]			
OME_{3-5} (kg)	1.00	1.00	1.00
CO_2 (kg)	9.75×10^{-2}	6.83×10^{-2}	1.12
CO (kg)	6.21×10^{-5}	6.21×10^{-5}	6.45×10^{-5}
Methane	—	3.72×10^{-4}	2.35×10^{-6}
Formaldehyde, air (kg)	1.55×10^{-5}	5.35×10^{-5}	1.56×10^{-5}
Methanol, air (kg)	3.83×10^{-3}	3.06×10^{-5}	2.20×10^{-4}
NO_2 (kg)	6.75×10^{-5}	6.75×10^{-5}	1.18×10^{-7}
NO_x (kg)	2.36×10^{-4}	2.93×10^{-4}	3.14×10^{-4}
SO_x (kg)	—	5.69×10^{-5}	6.47×10^{-7}
NMVOC (kg)	1.86×10^{-6}	1.86×10^{-6}	1.86×10^{-6}
Particulates, > 2.5 μm and	3.10×10^{-6}	3.10×10^{-6}	3.34×10^{-6}
Acetaldehyde (kg)	—	—	1.18×10^{-9}
Acetic acid (kg)	—	—	1.76×10^{-7}
Benzene (kg)	—	—	4.71×10^{-7}
Benzo(a) pyrene (kg)	—	—	1.18×10^{-11}
Butane (kg)	—	—	8.24×10^{-7}
Mercury (kg)	—	—	3.53×10^{-11}
PAH, polycyclic aromatic hydrocarbons (kg)	—	—	1.18×10^{-8}
Pentane (kg)	—	—	1.41×10^{-6}
Propane (kg)	—	—	2.35×10^{-7}
Propionic acid (kg)	—	—	2.35×10^{-8}
Toluene (kg)	—	—	2.35×10^{-7}
BOD5, biological O_2 demand, water (kg)	4.96×10^{-6}	7.33×10^{-5}	5.34×10^{-6}
COD, chemical O_2 demand, water (kg)	4.96×10^{-6}	1.91×10^{-4}	1.91×10^{-4}
DOC, dissolved organic C, water (kg)	—	9.11×10^{-5}	9.11×10^{-5}
AOX, absorbable organic halogen as Cl (kg)	—	3.79×10^{-7}	3.79×10^{-7}
Chloride, water (kg)	—	7.59×10^{-7}	7.59×10^{-7}
Formaldehyde, water (kg)	—	—	3.79×10^{-5}
Methanol, water (kg)	—	—	1.14×10^{-5}
Phenol, water (kg)	—	3.79×10^{-6}	3.79×10^{-6}
Phosphorus, water (kg)	—	3.79×10^{-6}	3.79×10^{-6}
Suspended solids, water (kg)	—	7.59×10^{-6}	7.59×10^{-6}
Total organic carbon (kg)	—	9.11×10^{-5}	9.11×10^{-5}
Catalyst waste (kg)	3.10×10^{-5}	3.10×10^{-5}	3.10×10^{-5}
Wastewater (m^3)	3.31×10^{-4}	1.14×10^{-4}	2.13×10^{-3}

[a] Inventory based on the work by Hank *et al.*,[13] Wernet *et al.*,[41] Singh *et al.*[42] and González-Garay *et al.*[43] [b] Unspecified sub-compartment is applied to all of the emissions. This also applies for the inventories included in the ESI.

2.2.2.1 CO_2 alternatives (SS1). DAC is the only monofunctional process for CO_2 supply. Inventory data for the DAC process (Table S2†) are taken from the work by Keith *et al.*,[44] which correspond to a KOH absorbent coupled with a calcium caustic recovery loop. In particular, the CO_2 from DAC is represented as a negative flow.

The biogas scenario captures CO_2 from the anaerobic digestion of sewage sludge. Sewage sludge from municipal wastewater facilities is converted by mesophilic bacteria into biomethane and CO_2. This biogas is then upgraded to biomethane, which can be injected into the natural gas grid, while an extra cleaning step reduces the H_2S content in the CO_2 stream to levels compatible with the downstream catalytic processes. Inventory data for this process (Table S3†) are taken from the work by Hank *et al.*[13] The production cost (PC) used to compute the allocation factor for biomethane is taken from the literature;[45] while the allocation factor for CO_2 is derived from a Sherwood correlation for the cost of CO_2 from industrial gas streams.[1,46]

The ammonia scenario entails the capture of CO_2 from ammonia production. This classical process involves the steam reforming of natural gas to produce a mixture containing mainly CO_2, N_2 and H_2 that undergoes CO_2 separation by absorption with monoethanolamine (MEA). Ammonia is then produced by reacting H_2 and N_2 with an iron-based catalyst. The inventory data (Table S4†) are taken from Hank *et al.*[13] For the economic allocation, the PC of CO_2 is again estimated using a Sherwood correlation,[1] while the PC of ammonia is taken from the literature.[47]

The power plant scenario involves the procurement of CO_2 from coal- or gas-fired power plants. In both processes, the post-combustion CO_2 capture relies on a conventional absorption process with MEA as the solvent. The inventory data (Tables S5 & S6†) are taken from González-Garay *et al.*[43] and Singh *et al.*[42] for coal- and gas-fired power stations, respectively. The corresponding allocation factors are based on the electricity price and the production cost of CO_2 capture.[43]

2.2.2.2 H_2 alternatives (SS2). The electrolytic process for H_2 production relies on a polymer electrolyte membrane (PEM) consuming 52.6 kWh of electricity per kg of H_2 produced at 30 bar.[43] This high electricity consumption is the main driver of environmental impacts.[48] Notice that high-pressure operation favours the energy efficiency of the system, as pressurised H_2 is required in the methanol synthesis step downstream. It is furthermore assumed that any electrolytic oxygen produced (8 kg O_2 per kg H_2) is vented to the atmosphere. These methodological choices are consistent with the current state-of-the-art in LCA of hydrogen energy systems.[49] The resulting inventories for electrolytic H_2 with electricity from either nuclear, solar or wind can be found in Table S1.†

2.2.2.3 OME_{3-5} production (SS3). The feedstock to this subsystem is dependent on the methanol production pathway, which involves either CO_2 hydrogenation, SMR or BTM (Fig. 2). Heat integration is considered across the production stages of methanol, formaldehyde and OME_{3-5}.

The inventory data for CO_2 hydrogenation to methanol (Table S7†) is based on the work by González-Garay *et al.*,[43] where CO_2 and H_2 react in the presence of a Cu–ZnO–Al_2O_3 catalyst to yield a mixture of methanol and water with unconverted CO_2, H_2 and CO. Then, methanol is separated from the mixture by two flash units in series and a distillation column. This process provides an excess of steam, which is transferred to the OME_{3-5} process to satisfy part of its steam demand. The inventory data for the SMR and BTM routes (Tables S8 & S9†) are provided by ecoinvent.[41]

The inventory data for the production of formaldehyde (Table S10†) are based on the water ballast process developed by BASF for the complete conversion of methanol to aqueous formaldehyde in the presence of a silver-based catalyst.[41,50,51] Like the CO_2 hydrogenation route, this process generates extra steam that can be used to (partially) cover the heat requirements of the OME_{3-5} synthesis.

The production of OME_{3-5} proceeds by reacting methanol with aqueous formaldehyde on a sulfonic acid resin-based catalyst. The mixture of OME_n oligomers from the reactor is separated into different lengths *via* distillation. Oligomers with $n < 3$ or $n > 5$ are recycled back to the reactor in order to increase the yield of OME_{3-5}, which is the desired and only product in this stage.[7] Table 2 includes the inventory data for OME_{3-5} produced from methanol obtained *via* $H_2 + CO_2$, SMR or BTM.

2.2.2.4 Fuel distribution and utilization (SS4). The final subsystem entails the distribution of OME_{3-5} to gas stations and its utilization in diesel vehicles (Fig. 2). Distribution is highly variable, since it depends on the geographical location. A distribution transport system combining lorry, train and ship over a total distance of 400 km is assumed herein.[13] The utilization phase involves the combustion of OME_{3-5} in compression ignition engines, assuming a fuel consumption of 2.37 MJ km^{-1} based on the model "transport, passenger car, medium size, diesel, EURO 5" within ecoinvent.[41]

The lower energy content of OME_{3-5} compared to diesel results in a higher fuel consumption in compression ignition engines. Experimental studies have shown that the consumption of diesel can be *cf.* 46% lower than that of OME_{3-5}, while OME_{3-5} presents a small efficiency improvement of 1–3% concurrently. Diesel consumption (m_{Diesel}) is set to 0.0528 kg km^{-1},[52] while OME_{3-5} consumption is estimated from:

$$m_{OME_{3-5}} = m_{Diesel} \frac{LHV_{Diesel}}{LHV_{OME_{3-5}}} (1 - \eta) \quad (1)$$

with the lower heating values $LHV_{Diesel} = 42.8$ MJ kg^{-1} and $LHV_{OME_{3-5}} = 19.0$ MJ kg^{-1}, and assuming an average efficiency improvement η of 2%. The inventory data associated to the distribution and utilization phase are reported in Tables S11 & S12,† respectively.

2.2.3 Environmental impact assessment. The selected LCIA method is ReCiPe2016,[53] a harmonized method that provides characterization factors at the midpoint and endpoint levels, connected to each other through the so-called damage pathways. Midpoint and endpoint impacts focus on different stages of the cause-effect chain. The former comprises 18 different impact categories, while endpoint impact categories represent the three areas of protection of human health damage, damage to ecosystems quality, and resource scarcity. Human health is

measured in disability-adjusted life-years (DALY) and quantifies the burden of human disease caused by environmental damage. Ecosystems quality quantifies the local species loss integrated over time, measured in species × year. Resource scarcity quantifies the future extra costs, in USD 2013, associated with fossil and mineral extraction.[53] Both levels are complementary as the midpoint categories have a more direct relation with the environmental flows and present a lower uncertainty; while interpreting the environmental flows is both simpler and more direct at the endpoint level. The results hereafter correspond mainly to characterization factors at the endpoint level, but other results employing midpoint characterization factors are reported in the ESI (Fig. S1†). The assessment relies on the hierarchist perspective, which is based on the cultural theory of scientific agreement and adopts a medium time-frame of 100 years for the environmental effects.[54]

Alongside quantifying the environmental impacts, our assessment considers their monetary valuation as externalities, or monetization in short. This procedure translates the endpoint environmental burdens into monetary units, thereby enabling their direct comparison.[55,56] It has been applied to the environmental assessment of chemical processes such as methanol,[43] propylene[57] and ionic liquids for biomass pretreatment.[58] The conversion factors proposed by Weidema[56] are used herein (Table S13†).

2.3 Economic assessment

A simplified economic assessment is conducted based on the driving cost (DC; eqn (2)),[12] which consists of the total annualised cost (TAC)—often used in the economic assessment of chemical processes—and the distribution cost (C_{dist}). The TAC (eqn (3)) comprises the OPEX, the annualized CAPEX, and other miscellaneous costs, including costs for laboratory analysis and wastewater and waste gas treatment. The OPEX (eqn (4)) represents the cost involved in maintaining a chemical facility in operation (directly related to the production volume), including costs of raw materials (C_{rm}), utilities (C_u) and personnel (C_p).[59,60] Moreover, the personnel costs assume two facilities—one for methanol and formaldehyde, and the other for OME_{3-5}—each one employing three operators in four rotating shifts with a salary of 50 000 USD per operator shift year.[60] The CAPEX (eqn (5)) involves all the costs associated with building a chemical facility, here estimated as 22.5% of the investment cost (IC; eqn (6)). This expression allows to compute the inside battery limits (ISBL) investment cost of the OME_{3-5} process (C_{OME3-5}) with a defined capacity $S_{OME3-5} = 40$ kton per year based on an existing reference process with the same or similar technology, and with known ISBL investment cost (C_{ref}) and capacity (S_{ref}). It has been reported that since the OME_{3-5} process is governed by distillation operation units, it may be assimilated to a typical oil refinery process with $S_{ref} = 5000$ kton per year, $C_{ref} = 780$ MUSD,[12] and a regression capacity factor α of 0.7.[60] The miscellaneous costs are estimated at 5% of the OPEX and CAPEX. Table S14† includes all the prices and costs required for computing the economic indicator associated with the OME_{3-5} alternatives.

$$DC = TAC + C_{dist} \quad (2)$$

$$TAC = OPEX + CAPEX + Misc. \quad (3)$$

$$OPEX = C_{rm} + C_u + C_p \quad (4)$$

$$CAPEX = 0.225 \times IC \quad (5)$$

$$IC = C_{OME_{3-5}} = C_{ref}\left(\frac{S_{OME_{3-5}}}{S_{ref}}\right)^{\alpha} \quad (6)$$

3 Results and discussions

The assessment of all 17 OME_{3-5} production pathways was conducted in SimaPro (version 9.0), using ecoinvent 3.5 (ref. 41) as the background database and ReCiPe2016 (ref. 53) as the impact assessment method.

3.1 Global warming

Fig. 3 compares the GW impact of the 17 pathways against conventional diesel. The results are arranged top-to-bottom in ascending order of impacts (from the most to the least favourable option) and comprise a break down into main inventory flow contributions. Recall that CO_2 from DAC is accounted for as a negative emission, whereas CO_2 emitted by the BTM process is modelled as a biogenic source and other CO_2 emissions associated with fossil raw materials are accounted for with positive fossil characterization factors.

The tailpipe emissions represent the highest individual contribution in all of the scenarios but OME_{BTM}, with an impact of 0.17 and 0.20 kg CO_2e per km for diesel and the OME fuels, respectively. The greater GW impact associated with the use of OME fuels is attributed to their lower energy content, which is detrimental to fuel economy. Notice that in the OME_{BTM} case,

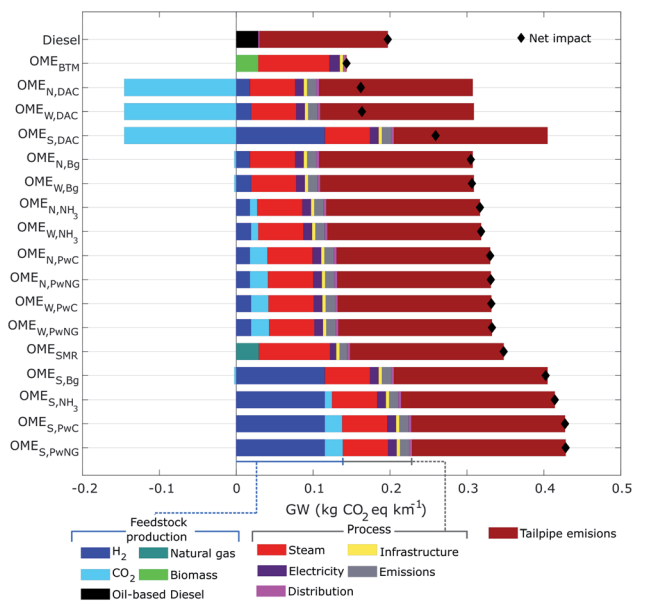

Fig. 3 Breakdown of the global warming (GW) impact for the fuels.

both process and tailpipe emissions contribute marginally due to the biogenic carbon origin.

The largest global warming impact corresponds to the group of solar-based fuels ($OME_{S,PwNG}$, $OME_{S,PwC}$, $OME_{S,NH3}$, and $OME_{S,Bg}$) with an average of 0.42 kg CO_2e per km. This unfavourable performance is mainly attributed to the manufacture of Si-based photovoltaic panels that supply electricity for electrolytic H_2 production.

The extra consumption of natural gas to meet the heat demand of the OME_{3-5} process (Fig. 2) is the main driver for the unfavourable performance of the OME_{SMR} fuel as well as the nuclear- and wind-based OME fuels ($OME_{W,PwNG}$, $OME_{W,PwC}$, $OME_{N,PwNG}$, $OME_{N,PwC}$, $OME_{W,NH3}$, $OME_{N,NH3}$, $OME_{W,Bg}$, $OME_{N,Bg}$), with an average value of 0.32 kg CO_2e per km. In comparison, $OME_{S,DAC}$, diesel, and $OME_{W,DAC}$ fuels have an estimated GW impact of 0.26, 0.20 and 0.16 kg CO_2e per km, respectively. Finally, the most favourable fuel within the GW impact category is OME_{BTM} with 0.14 kg CO_2e per km, that is, 65% and 58% less than the solar and SMR based technologies and 30% less than conventional diesel. These results are in agreement with other studies reporting lower GW impact for OME_{3-5} produced from electrolysis-based hydrogen and CO_2 captured from air, ammonia plants, or biogas,[13] despite some differences due to the allocation method employed to account for multi-functionality in the CO_2 systems and the electricity mix used to power the electrolyzers in H_2 production.

Similar comparisons are presented in Fig. S1† for midpoint impact categories other than GW. These midpoint impacts can be used to identify the main damage mechanisms affecting the endpoint protection areas of human health, ecosystems quality, and resource scarcity that are detailed below.

3.2 Human health

Fig. 4 compares the OME_{3-5} pathways with the diesel reference case under the protection area of human health (HH). These impacts are expressed in DALY per km travelled and the results are broken down by process stage. With about 2.5×10^{-7} DALY per km, fossil-based diesel outperforms all 17 OME_{3-5} fuel candidates, which increase the HH impact by 0.5–3.5 fold. Similar to the GW impact (Fig. 3), solar-based OME_{3-5} fuels ($OME_{S,PwNg}$, $OME_{S,PwC}$, $OME_{S,NH3}$, $OME_{S,Bg}$, $OME_{S,DAC}$) present the highest HH impact, with an average of 8.0×10^{-7} DALY per km. Following this are the OME_{SMR} fuel and the nuclear- and wind-based OME_{3-5} fuels, with an estimated average impact of 5.2×10^{-7} DALY per km. Finally, with a predicted 3.7×10^{-7} DALY per km, OME_{BTM} presents the lowest HH impact among all 17 OME_{3-5} candidates.

The feedstock production activity contributing the largest share of the HH protection area is solar-based H_2. This is attributed to manufacturing of the photovoltaic solar panels that power the electrolyzers, which impose large burdens on the midpoint impact categories of terrestrial ecotoxicity, human non-carcinogenic toxicity, GW and land use (see Fig. S1†). Nuclear- and wind-based H_2 production also carry large burdens. In contrast, the CO_2 procurement activities contribute the smallest share—being even a negative contribution in the case of DAC.

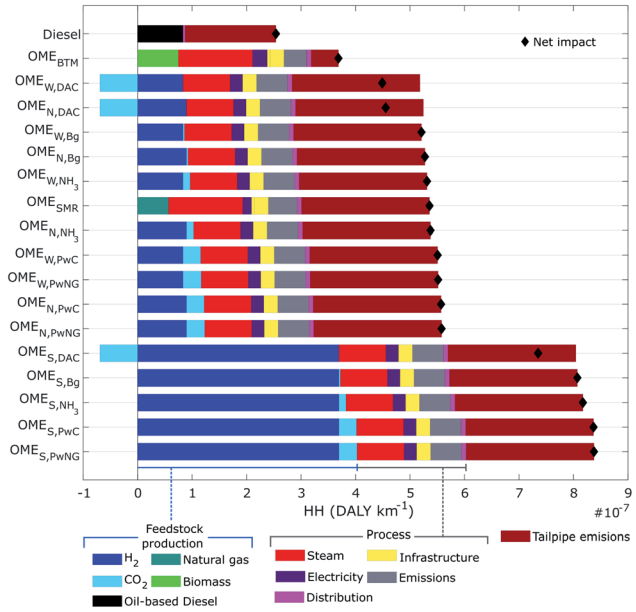

Fig. 4 Breakdown of the human health (HH) impact for the fuels.

With regards to process activities, steam presents the highest HH impact, followed by direct emissions, infrastructure and electricity. The impact of steam production is attributed to the natural gas used to provide heat to the OME_{3-5} distillation as well as the reformer in the SMR and BTM scenarios. The impact of direct emissions is caused by the waste gasses released at each step of the OME_{3-5} production.

Excepting only OME_{BTM}, tailpipe emissions are a major contributor to the HH impact of all the fuels. And the lower fuel economy of OME_{3-5} compared to diesel exacerbates the problem, in a similar way to the GW impact (Fig. 3). The impact of the biomass-derived OME_{3-5} (OME_{BTM}), is much lower in reason of the biogenic carbon emissions.

3.3 Ecosystems quality

Fig. 5 depicts the breakdown for the second protection area of ecosystems quality (EQ), where the impacts are expressed in species × year per km travelled. Notable differences exist between the OME_{3-5} fuel alternatives and the diesel reference case similar to the HH impact category. OME_{BTM} places by far the greatest burden on ecosystems with an estimated impact of 3.8×10^{-9} species × year per km, followed by the solar-based options with an average impact of 2.0×10^{-9} species × year per km. The OME_{SMR} and the group of nuclear- and wind-based OME_{3-5} fuels come next with an average impact of 1.2×10^{-9} species × year per km. Finally, with an estimated 0.7×10^{-9} species × year per km fossil-based diesel outperforms all of the OME_{3-5} fuel candidates within the EQ protection area by 1.5–6 fold.

With regards to feedstock production activities, the impact of biomass production alone on ecosystems is greater than the impact of any other fuel. This can be explained by the very large burden placed on land use for growing biomass (Fig. S1†). The manufacturing of solar panels is again a major bottleneck for solar-based H_2 production, with an average share of 45% of the

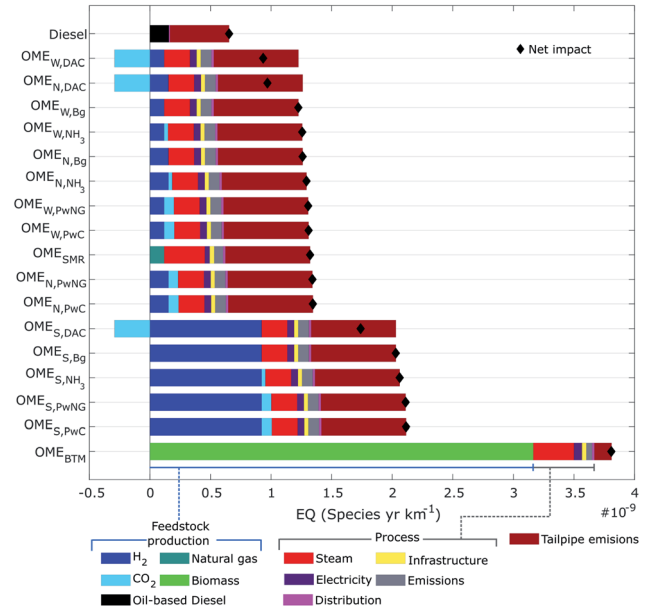

Fig. 5 Breakdown of the ecosystems quality (EQ) impact for the fuels.

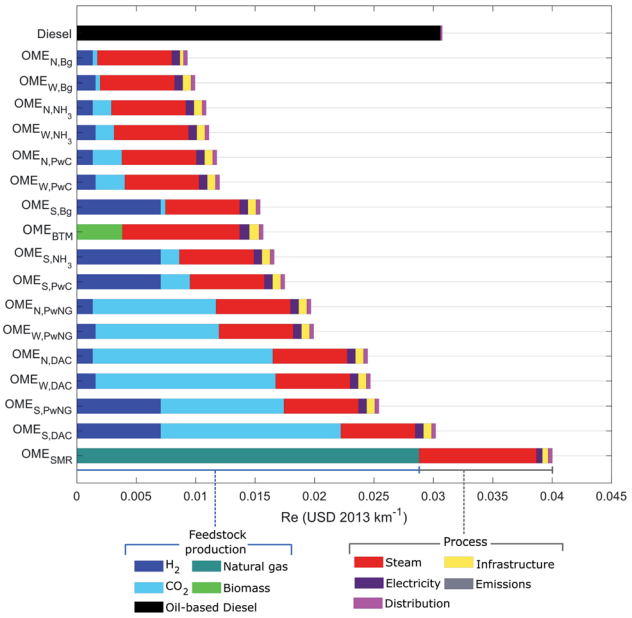

Fig. 6 Breakdown of the resource scarcity (Re) impact for the fuels.

total EQ impact. The remaining feedstocks (wind- and nuclear-based H_2, CO_2, and natural gas procurement) all have low or even negative contributions on the EQ protection area.

The EQ impacts associated with the process activities follow a similar pattern as the HH impact category. Steam is the largest contributor, followed by process emissions, electricity, and infrastructure to a lesser extent. Excepting only OME_{BTM}, tailpipe emissions place an important burden on EQ, making over 50% of the total impact in several scenarios. The lower EQ impact of diesel utilization compared to all OME_{3-5} alternatives is attributed to its better fuel economy.

3.4 Resource scarcity

The third protection area of resource scarcity (Re) quantifies the future extra costs associated to fossil-fuel and mineral extraction. Fig. 6 compares the Re impacts and their breakdowns, expressed in USD_{2013} per km travelled. The predictions in this area differ significantly from those in the HH and EQ categories. The largest contributors are OME_{SMR} and diesel with 0.04 and 0.03 USD_{2013} per km, respectively, followed by the OME fuels using CO_2 from DAC or gas-fired power plants ($OME_{S,DAC}$, $OME_{S,PwNG}$, $OME_{W,DAC}$, $OME_{N,DAC}$, $OME_{W,PwNG}$ and $OME_{N,PwNG}$) with Re impacts between 0.02–0.03 USD_{2013} per km. The most favourable fuel in this protection area is $OME_{N,Bg}$ with 0.009 USD_{2013} per km, which is four times lower than OME_{SMR}.

According to Fig. 6, the fuels that depend heavily on oil and natural gas are causing the highest Re impacts. The raw material in fossil-based diesel is of course oil. But the production of OME_{SMR} is heavily reliant on natural gas, both as raw material in the production of methanol and as energy source for steam production; the latter also applies to the other OME_{3-5} fuels. Solar-based H_2 and biomass also place large burdens on Re due to the use of natural gas and oil-based fuels in the manufacturing of photovoltaic solar panels and the production, distribution and pretreatment of biomass, respectively. Finally, the Re impact of CO_2 using DAC is attributed to the large share of natural gas (44%) in the UK electricity mix.[41,61]

These results comply with projections by the Energy Information Administration,[5] whereby oil and natural gas consumption are predicted to increase by 18% and 43%, respectively by 2040—making their reserves scarcer—while those of coal and nuclear materials will remain stable. The higher Re impacts for the scenarios where CO_2 is captured from gas-fired power plants compared to the scenarios where CO_2 is captured from coal-fired power plants are also in agreement with the projections for coal and natural gas resources. Finally, in the scenarios where CO_2 is obtained from biogas, the Re impact is low since the feedstock (sewage sludge) is a waste derived from anthropogenic activities.

3.5 Driving cost and monetized externalities

Turning to economic considerations, Fig. 7 shows the DC and its breakdown for all 17 OME fuels compared with the diesel reference case. The highest costs correspond to those OME_{3-5} fuels where H_2 is produced in solar-powered electrolyzers, with an average DC of 0.30 USD_{2019} per km. This is followed by the wind- and nuclear-based H_2 scenarios with an average DC of 0.19 USD_{2019} per km, and the BTM and SMR scenarios with 0.12 and 0.07 USD_{2019} per km, respectively. Finally, the fuel having the lowest DC is fossil-based diesel with around 0.05 USD_{2019} per km, which is 3–5 times less than the OME_{3-5} fuels relying on electrolysis for H_2 production.

The DC breakdown reveals that H_2 procurement is indeed the main cost driver for the OME_{3-5} fuels that rely on electrolysis, with 0.12–0.24 USD_{2019} per km and a corresponding share of over 60%. In terms of CO_2 procurement, DAC presents the largest cost around 0.03 USD_{2019} per km, which is due to the low atmospheric CO_2 concentration that renders the sequestration

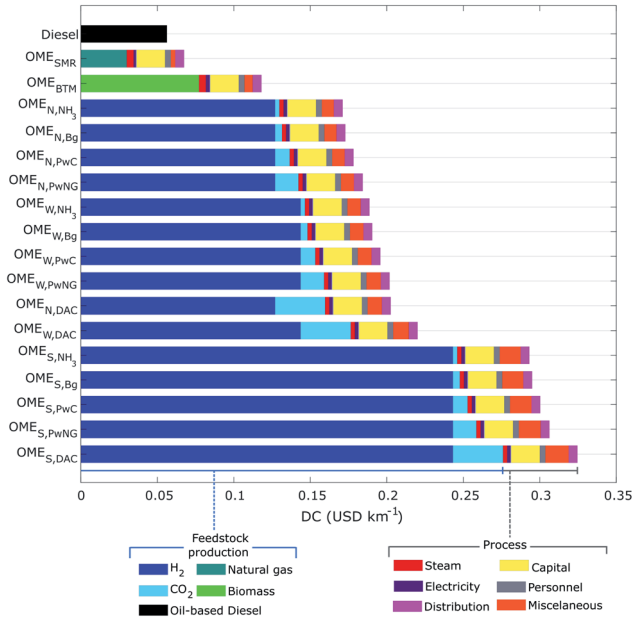

Fig. 7 Breakdown to the driving cost (DC) for the fuels.

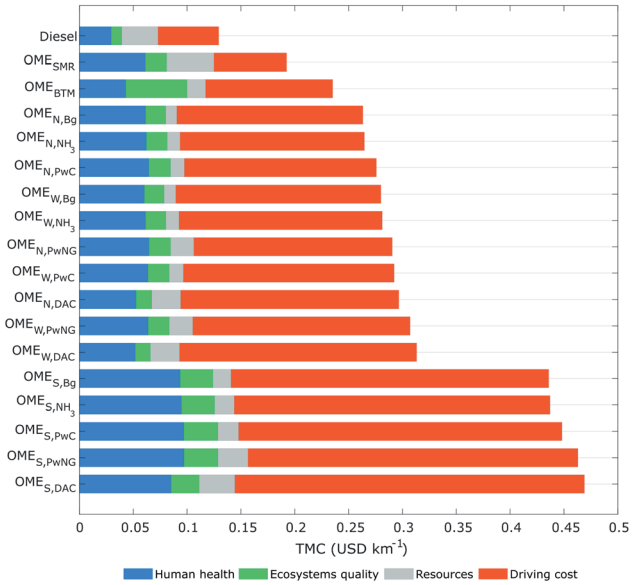

Fig. 8 Breakdown of the total monetized cost (TMC) for the fuels.

energy-intensive and costly. Naturally, the procurement of natural gas and biomass are major cost drivers for the OME_{SMR} and OME_{BTM} fuels as well.

The contribution of environmental externalities to the total monetised cost (TMC) of each fuel is presented in Fig. 8, expressed in USD_{2019} per km travelled. The TMC adds the predicted HH, EQ and Re externalities to the DC estimates. The largest TMC corresponds to the solar-based fuels with an average cost around 0.45 USD_{2019} per km, followed by the nuclear- and wind-based fuels averaging around 0.29 USD_{2019} per km, then OME_{BTM} and OME_{SMR} at 0.23 and 0.19 USD_{2019} per km, respectively. Overall, none of the OME_{3-5} fuel candidates present a lower TMC than the diesel reference case (0.13 USD_{2019} per km). Diesel even turns out to be less than half the TMC of any OME_{3-5} fuel produced from biomass or renewable H_2.

The DC makes up the largest contribution to the TMC in all the OME_{3-5} fuels relying on electrolysis because of the high procurement cost of H_2 (Fig. 7). Likewise, the procurement of natural gas or biomass makes up a large share of the TMC for both OME_{SMR} and OME_{BTM} alternatives. When considering only the environmental externalities, several OME fuels are predicted to be competitive against diesel nonetheless. For instance, estimated externalities around 0.09 USD_{2019} per km for the wind- or nuclear-based OME_{3-5} fuels are comparable to those of diesel (0.07 USD_{2019} per km).

3.6 Sensitivity of CO_2 allocation factors

Large uncertainty in the economic value of concentrated CO_2 justifies a sensitivity analysis of the predicted environmental burdens in terms of the economic allocation factor used for CO_2 in multi-functional subsystems (*cf.* Section 2.2.1). The variations in GW, HH, EQ and Re impacts corresponding to a price for concentrated CO_2 in the range 0–1000 USD per ton are reported on Fig. S2 in the ESI.†

The effects of this allocation uncertainty are comparable across the GW, HH and EQ categories. For those OME_{3-5} fuels relying on CO_2 captured from ammonia plants, the GW, HH and EQ impacts could increase by up to 50–60%; while the variation ranges predicted for CO_2 captured from gas- or coal-fired power plants or biogas from sewage sludge are much narrower. Notice also that none of the OME_{3-5} fuels outperform diesel in these categories, even in putting the greatest burdens on the biomethane, ammonia, and electricity co-products by decreasing the CO_2 allocation factors.

The allocation uncertainty has a somewhat different and larger effect on the Re impact category. The variation ranges for the OME_{3-5} fuels utilizing CO_2 captured from ammonia plants and gas-fired power plants are several times smaller or larger than the predicted Re impacts themselves. Notice, in particular, how the worst-case impacts—that is, with a concentrated CO_2 cost of 1000 USD per ton—of these OME_{3-5} fuels could exceed that of diesel even in the Re category. This result is expected insofar as these processes are heavily reliant on natural gas, the reserves of which are predicted to become scarcer in the near future.[5]

On the whole, it is worth noting that such large variations in the economic allocation factor for CO_2 do not lead to substantial variations in the TMC range of the OME_{3-5} fuels; comparable in magnitude to those observed on the HH and EQ impacts. None of the OME_{3-5} fuels outperform diesel even in the most favorable of scenarios. This is because the procurement of CO_2 only incurs a relatively small burden on the endpoint protection areas and the driving cost as part of the OME_{3-5} infrastructure (Fig. 2).

3.7 Discussions

Our results are in agreement with the conclusions of other studies comparing the environmental performance of OME_{3-5} and conventional diesel.[13] The general trend is a clear reduction

in GHG emissions for the OME_{3-5} fuels produced from biomass or using H_2 from nuclear- or wind-powered electrolysis and CO_2 from DAC. Conversely, the performance of such OME_{3-5} fuels in the midpoint impact categories of particulate matter, acidification and ozone formation is significantly worse than diesel, which is reflected through higher HH and EQ impacts.

The environmental and economic indicators considered herein present interesting trade-offs for most OME_{3-5} fuel candidates, excepting the solar-based alternatives. For instance, the biomass-based scenario has lower production costs but suffers from higher HH and EQ externalities. Conversely, the wind- and nuclear-based H_2 routes present lower EQ and HH impacts but show higher production costs. A breakdown of the corresponding impacts reveals that further efforts to reduce the environmental burdens—and thus the associated externalities—should be focused on H_2 production and, to a lesser extent, CO_2 capture. Under the assumptions made in this study, producing H_2 from wind- and nuclear-powered electrolysis and capturing CO_2 from biogas or using DAC constitute the most promising scenarios. Regarding wind-powered electrolysis, optimistic scenarios—namely, lower material and construction costs for wind turbines, capacity factor greater than 44%, and wind farms with class 4 winds or higher—predict a H_2 production cost as low as 3 USD per kg.[62] Capturing CO_2 from the biogas produced by digestion of sewage sludge is recommended since it imposes a low burden on all three protection areas. The DAC scenario also enjoys negative HH and EQ externalities but places a high burden on Re, which could be mitigated by switching to an electricity production mix with low share of natural gas and high share of renewables such as wind and hydroelectricity. Finally, the OME_{BTM} fuel benefits from lower H_2 production cost and lower global warming impact, but imposes a large burden on EQ. Improvement pathways include new catalysts for biomass gasification at lower temperatures and switching to energy crops such as poplar with higher efficiency, lower rotational times, and higher yields per cultivated area.[63] At the process level, optimization of the OME_{3-5} production process could determine process configurations and operational strategies with lower costs, for instance, by lowering the steam demand. Producing steam using renewable energy could also alleviate the environmental burden of OME_{3-5} fuels.

It is clear that our assessment is tainted by multiple sources of uncertainty, most prominently in the life-cycle inventory and economic data. Uncertainty on the LCI entries is related to data quality indicators such as completeness, reliability, temporal correlation, technological state, geographical correlation and sampling size. A key uncertainty on economic data is related to the feedstock price, including oil and natural gas which have shown a high historical volatility. Though not considered herein, such uncertainty quantification could build upon the present results in a follow-up study.

4 Conclusions

This paper has presented a comparative assessment of multiple OME_{3-5} production pathways using detailed life-cycle assessment and environmental impact monetization. Even though OME_{3-5} fuels derived from biomass or CO_2 captured from DAC could mitigate the GW impact by substituting conventional diesel, the analysis of a broad range of environmental and economic indicators has revealed significant trade-offs between the driving cost and the protection areas of human health and ecosystems quality. Only under the resource scarcity area do the OME_{3-5} fuel alternatives place a consistently lower burden on the future availability of fossil and mineral materials compared to conventional diesel. Overall, the total monetized cost of all 17 OME_{3-5} fuel candidates is 1.5–3.6 times that of conventional diesel. Their high driving cost suggests that the technology is not yet cost-competitive with conventional diesel. Though, when considering only the environmental externalities, several OME_{3-5} alternatives are predicted to be competitive against diesel—most prominently, those OME_{3-5} fuels that either use biomass as feedstock, or H_2 produced from wind- or nuclear-powered electrolysis and CO_2 captured from biogas or air.

Given that the raw materials contribute substantially to the total monetized cost, further research effort should be dedicated to sustainable H_2 production and CO_2 capture. The procurement cost of H_2 from wind-powered electrolysis could be reduced by optimising wind farms and developing more efficient electrolyzers. Both the production cost and environmental burden of syngas derived from biomass could be reduced by developing new catalysts for gasification under less severe operating conditions and applying process intensification strategies. The externalities of CO_2 capture could be reduced by using solvents with higher selectivity or lowering the energy demand for solvent regeneration. An increased share of renewables in the electricity mix could further reduce the environmental impact of energy-intensive processes such as DAC. Process intensification and optimization, finally, could improve the process designs and operations, for instance by reducing the plantwide steam consumption.

Our results, therefore, highlight the need for embracing impacts beyond climate change in the environmental assessment of alternative fuels and including negative externalities in their economic assessment. Although the predicted global warming impact of several OME_{3-5} fuels may be lower than conventional diesel, this benefit is indeed overturned after considering the externalities and production costs altogether. Our results also showcase the potential of integrating LCA with externality monetization and high-level process modelling in the holistic assessment of alternative fuels. This integrated approach could support decision- and policy-makers in the transition toward a more sustainable transport sector.

Conflicts of interest

There are no conflicts to declare.

Acknowledgements

Daniel F. Rodríguez-Vallejo acknowledges the financial support from the Colombian Administrative Department of Science

Technology and Innovation (COLCIENCIAS). Benoît Chachuat is grateful to the Engineering and Physical Sciences Research Council (EPSRC) for financial support under Grants EP/N010531/1 and EP/V011863/1.

References

1 P. Bains, P. Psarras and J. Wilcox, *Prog. Energy Combust. Sci.*, 2017, **63**, 146–172.
2 World Resources Institute, *Everything You Need to Know About the Fastest-Growing Source of Global Emissions: Transport*, 2019, https://www.wri.org, accessed: 2020-07-14.
3 IPCC, *Climate Change 2014: Mitigation of Climate Change. Contribution of Working Group III to the Fifth Assessment Report of the Intergovernmental Panel on Climate Change*, 2014.
4 IEA, *Tracking Transport 2020*, 2020, www.iea.org/reports/tracking-transport-2020, accessed: 2020-07-14.
5 J. Conti, P. Holtberg, J. Diefenderfer, A. LaRose, J. T. Turnure and L. Westfall, *International energy outlook 2019 with projections to 2050*, Energy Information Administration (EIA), Washington DC, US technical report, 2016.
6 S. Deutz, D. Bongartz, B. Heuser, A. Kätelhön, L. S. Langenhorst, A. Omari, M. Walters, J. Klankermayer, W. Leitner, A. Mitsos, *et al.*, *Energy Environ. Sci.*, 2018, **11**, 331–343.
7 N. Schmitz, E. Ströfer, J. Burger and H. Hasse, *Ind. Eng. Chem. Res.*, 2017, **56**, 11519–11530.
8 J. Liu, H. Wang, Y. Li, Z. Zheng, Z. Xue, H. Shang and M. Yao, *Fuel*, 2016, **177**, 206–216.
9 J. Tian, Y. Cai, Y. Shi, Y. Cui and R. Fan, *International Journal of Automotive Technology*, 2019, **20**, 277–288.
10 M. Härtl, K. Gaukel, D. Pélerin and G. Wachtmeister, *MTZ Worldwide*, 2017, **78**, 52–59.
11 D. Pélerin, K. Gaukel, M. Härtl, E. Jacob and G. Wachtmeister, *Fuel*, 2020, **259**, 116231.
12 N. Schmitz, J. Burger, E. Ströfer and H. Hasse, *Fuel*, 2016, **185**, 67–72.
13 C. Hank, L. Lazar, F. Mantei, M. Ouda, R. J. White, T. Smolinka, A. Schaadt, C. Hebling and H.-M. Henning, *Sustainable Energy Fuels*, 2019, **3**, 3219–3233.
14 International Organization for Standardization, *Environmental Management: Life Cycle Assessment; Principles and Framework*, ISO, 2006.
15 International Organization for Standardization, *Environmental Management: Life Cycle Assessment; Requirements and guidelines*, ISO, 2006.
16 G. J. Ruiz-Mercado, A. Carvalho and H. Cabezas, *ACS Sustainable Chem. Eng.*, 2016, **4**, 6208–6221.
17 G. Guillen-Gosalbez, J. A. Caballero and L. Jimenez, *Ind. Eng. Chem. Res.*, 2008, **47**, 777–789.
18 C. Pieragostini, M. C. Mussati and P. Aguirre, *J. Environ. Manage.*, 2012, **96**, 43–54.
19 I. E. Grossmann and G. Guillén-Gosálbez, *Comput. Chem. Eng.*, 2010, **34**, 1365–1376.
20 J. Clavreul, D. Guyonnet and T. H. Christensen, *Waste Manage.*, 2012, **32**, 2482–2495.
21 D. Bongartz and A. Mitsos, *Journal of Global Optimization*, 2017, **69**, 761–796.
22 X. Zhang, A. Kumar, U. Arnold and J. Sauer, *Energy Procedia.*, 2014, **61**, 1921–1924.
23 C.-Y. Chung and I.-L. Chien, *IFAC-PapersOnLine*, 2018, **51**(18), 578–583.
24 J.-O. Weidert, J. Burger, M. Renner, S. Blagov and H. Hasse, *Ind. Eng. Chem. Res.*, 2017, **56**, 575–582.
25 C. F. Breitkreuz, N. Schmitz, E. Ströfer, J. Burger and H. Hasse, *Chem. Ing. Tech.*, 2018, **90**, 1489–1496.
26 D. Bongartz, J. Burre and A. Mitsos, *Ind. Eng. Chem. Res.*, 2019, **58**, 4881–4889.
27 J. Burre, D. Bongartz and A. Mitsos, *Ind. Eng. Chem. Res.*, 2019, **58**, 5567–5578.
28 R. H. Boyd, *J. Polym. Sci.*, 1961, **50**, 133–141.
29 M.-r. Kang, H.-y. Song, F.-x. Jin and C. Jing, *J. Fuel Chem. Technol.*, 2017, **45**, 837–845.
30 J. Burger, M. Siegert, E. Ströfer and H. Hasse, *Fuel*, 2010, **89**, 3315–3319.
31 J.-O. Drunsel, M. Renner and H. Hasse, *Chem. Eng. Res. Des.*, 2012, **90**, 696–703.
32 D. Oestreich, L. Lautenschütz, U. Arnold and J. Sauer, *Chem. Eng. Sci.*, 2017, **163**, 92–104.
33 N. Schmitz, J. Burger and H. Hasse, *Ind. Eng. Chem. Res.*, 2015, **54**, 12553–12560.
34 B. Li, Y. Li, H. Liu, F. Liu, Z. Wang and J. Wang, *Applied Energy*, 2017, **206**, 425–431.
35 A. Azapagic and R. Clift, *Comput. Chem. Eng.*, 1999, **23**, 1509–1526.
36 N. von der Assen, J. Jung and A. Bardow, *Energy Environ. Sci.*, 2013, **6**, 2721–2734.
37 L. J. Müller, A. Kätelhön, M. Bachmann, A. Zimmermann, A. Sternberg and A. Bardow, *Frontiers in Energy Research*, 2020, **8**, 15.
38 N. von der Assen, P. Voll, M. Peters and A. Bardow, *Chem. Soc. Rev.*, 2014, **43**, 7982–7994.
39 E. A. Quadrelli, G. Centi, J.-L. Duplan and S. Perathoner, *ChemSusChem*, 2011, **4**, 1194–1215.
40 E. A. Quadrelli and G. Centi, *ChemSusChem*, 2011, **4**, 1179–1181.
41 G. Wernet, C. Bauer, B. Steubing, J. Reinhard, E. Moreno-Ruiz and B. Weidema, *Int. J. Life Cycle Assess.*, 2016, **21**, 1218–1230.
42 B. Singh, A. H. Strømman and E. Hertwich, *Int. J. Greenhouse Gas Control*, 2011, **5**, 457–466.
43 A. González-Garay, M. S. Frei, A. Al-Qahtani, C. Mondelli, G. Guillén-Gosálbez and J. Pérez-Ramírez, *Energy Environ. Sci.*, 2019, **12**, 3425–3436.
44 D. W. Keith, G. Holmes, D. S. Angelo and K. Heidel, *Joule*, 2018, **2**, 1573–1594.
45 The International Renewable Energy Agency, *Road transport: The cost of renewable solutions*, IRENA, 1st edn, 2013.
46 K. Z. House, A. C. Baclig, M. Ranjan, E. A. van Nierop, J. Wilcox and H. J. Herzog, *Proc. Natl. Acad. Sci. U. S. A.*, 2011, **108**, 20428–20433.
47 U. G. Survey, *Mineral commodity summaries 2016*, U.S. Geological Survey, Reston, Virginia, U.S, 1st edn, 2016.

48 A. Valente, D. Iribarren and J. Dufour, *Int. J. Life Cycle Assess.*, 2017, **22**, 346–363.
49 A. Valente, D. Iribarren and J. Dufour, *Sci. Total Environ.*, 2021, **756**, 144132.
50 M. Bohnet, *Ullmann's encyclopedia of industrial chemistry*, Wiley-Vch, 2003.
51 M. Qian, M. Liauw and G. Emig, *Appl. Catal., A*, 2003, **238**, 211–222.
52 A. Simons, *Int. J. Life Cycle Assess.*, 2016, **21**, 1299–1313.
53 M. A. Huijbregts, Z. J. Steinmann, P. M. Elshout, G. Stam, F. Verones, M. Vieira, M. Zijp, A. Hollander and R. van Zelm, *Int. J. Life Cycle Assess.*, 2017, **22**, 138–147.
54 J. Clavreul, H. Baumeister, T. H. Christensen and A. Damgaard, *Environmental Modelling & Software*, 2014, **60**, 18–30.
55 M. Pizzol, B. Weidema, M. Brandão and P. Osset, *J. Cleaner Prod.*, 2015, **86**, 170–179.
56 B. P. Weidema, *J. Ind. Ecol.*, 2015, **19**, 20–26.
57 D. F. Rodríguez-Vallejo, G. Guillén-Gosálbez and B. Chachuat, *ACS Sustainable Chem. Eng.*, 2020, **8**, 3072–3081.
58 H. Baaqel, I. Díaz, V. Tulus, B. Chachuat, G. Guillén-Gosálbez and J. P. Hallett, *Green Chem.*, 2020, **22**, 3132–3140.
59 R. Turton, R. C. Bailie, W. B. Whiting and J. A. Shaeiwitz, *Analysis, Synthesis and Design of Chemical Processes*, Pearson Education, New Jersey, 2008.
60 R. K. Sinnott, *Chemical Engineering Design*, Elsevier, Amsterdam, 2014, vol. 6.
61 R. Itten, R. Frischknecht, M. Stucki and P. Scherrer, *Life cycle inventories of electricity mixes and grid*, 2012.
62 G. Saur and T. Ramsden, *Wind electrolysis: hydrogen cost optimization*, National Renewable Energy Laboratory (NREL), Golden, CO (United States, technical report, 2011.
63 C. M. Gasol, X. Gabarrell, A. Anton, M. Rigola, J. Carrasco, P. Ciria and J. Rieradevall, *Biomass Bioenergy*, 2009, **33**, 119–129.